# INITIAL PARAMETERS FOR STUDY 2

# DESIGN A

DRAFT 4

R.B. Palmer, S. Berg, R. Fernow, Y. Fukui,
J Gallardo, C. Kim, E. Kim, H. Kirk, J. Miller,
N. Mokhov, G. Penn, R. Weggel, J. Wurtele
8/25/00

## Abstract

The parameters are given for the front end of a neutrino factory (design A for Feasibility Study 2). No RF is employed near the target and relatively little polarization (22 %) is achieved, but the efficiency of producing muons is good ($\approx 0.2$ $\mu$/p with 24 GeV proton bunches with 3 ns rms length). Per MW of proton power, this is 7.4 $\times$ the performance of Feasibility Study 1.

The high efficiency is achieved by

1) using a liquid mercury target;

2) using two induction linacs and long drifts to achieve near non-distorting phase rotation. The final muons are distributed over 300 ns with a relatively uniform energy spread; and

3) tapering the focus strength in the cooling system so that the angular spread of the muons being cooled is maintained at a near constant value.

# Contents

# 1 Introduction

This note gives starting specifications and some simulation results for a first (Design A) design of a Feasibility Study 2 neutrino factory. It is a design that does not use low frequency rf near the target, has relatively little polarization, and requires proton pulses only $\leq 3$ ns.

This document can be found at:

http://pubweb.bnl.gov/people/palmer/nu/study2/paramsA.ps

and the tex files that made it at:

http://pubweb.bnl.gov/people/palmer/nu/study2/tex

The ICOOL files to simulate this design can be found at:

http://pubweb.bnl.gov/people/palmer/nu/study2/icoolA/

Later, and distinct, designs could include:

- Design B: using low frequency RF to obtain polarization, but that will require shorter proton bunches;
- Design C: a design with an agreed lower muon rate, but with less induction linac, cooling etc. to reduce cost;
- Design D: a design with emittance exchange and higher performance.

The scheme is illustrated in the following figure:

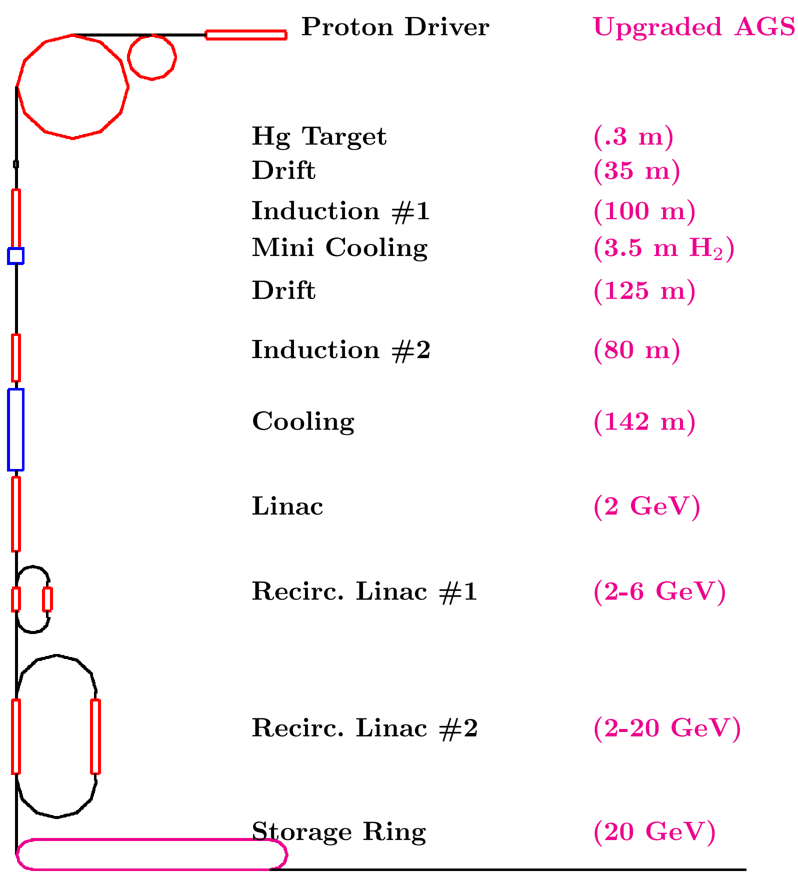


**c: aaprog scheme nupict.td**

The axial B fields along the system are shown:

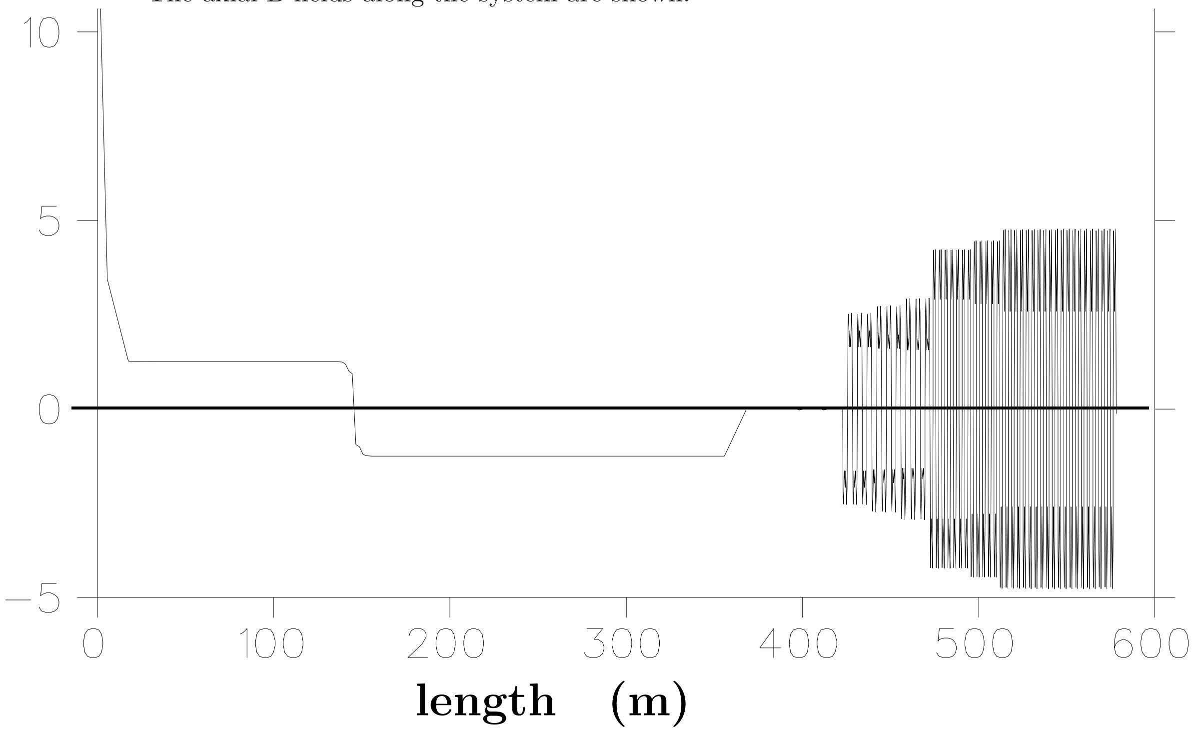


The axial field is 20 T at the target and tapers down to 1.25 T over 18 m. The field is reversed between the two halves of the hydrogen "mini-cooling" absorber at about 150 m. At 370 m there is a match from the -1.25 T fixed field to a lattice consisting of 2.75 m cells. There is another match at 480 m to a shorter cell (1.65 m).

The lengths of the components in the "Front End", up to the muon accelerators, are listed in the following table:

| | length m | totals m |
|---|---|---|
| target | 0.3 | 0.3 |
| taper | 17.6 | 17.9 |
| drift | 18 | 35.9 |
| Induction 1 | 100 | 135.9 |
| Drift | 5 | 140.9 |
| Mini-Cool | 10 | 150.9 |
| Drift | 125 | 275.9 |
| Induction 2 | 80 | 355.9 |
| Match to Super FOFO | 17.5 | 373.4 |
| Buncher | $20 \times 2.75 = 55$ | 428.4 |
| cooling part 1 | $18 \times 2.75 = 49.5$ | 477.9 |
| cooling part 2 | $56 \times 1.65 = 92.4$ | 570.3 |

The accelerators and storage ring will be specified later

# 2 Specifications

## 2.1 Proton driver

| | | |
|---|---|---|
| Energy | 24 | GeV |
| protons per bunch | $\approx 1.7\ \ 10^{13}$ | |
| bunches per fill | 6 | |
| time between extracted bunches | $\approx 20$ | ms |
| repetition rate | 2.5 | Hz |
| rms bunch length | $\leq 3$ | ns |
| beam power | $\geq 1$ | MW |

Finite time between bunches is required for a number of reasons:

- To allow time to refill the RF cavities in the accelerating systems and avoid excessive beam loading;
- To avoid the need for multi pulsing of the induction linacs; and
- to allow the liquid target to be re-established after its assumed dispersal by the previous bunch. It is this requirement that sets the minimum spacing: The time required depends on the jet velocity and other parameters, and is not yet known. The number of 20 ms is a reasonable starting assumption. An even separation of bunches at 15 Hz would also be even better, but would require an accumulator ring.

The possibility of an average power greater than 1 MW, up to 1.5 MW should also be considered. This would correspond to the average power assumed in

Feasibility Study 1.

## 2.2 Target

| | | |
|---|---|---|
| material | mercury | |
| velocity | $\approx 20$ | m/sec |
| length | 30 | cm |
| diameter | 1 | cm |
| angle to muon axis | 100 | mrad |
| displacement of front from axis | $\approx 1$ | cm |

A single proton bunch will heat the liquid to a temperature above its boiling point and generate substantial shock pressures. It is not believed that these will have significant adverse consequences, but, if it did, liquid lead/tin eutectic could be used. A graphite target (as used in study 1) could also be considered as a backup, but would reduce the neutrino intensity by a factor of 1.9 (see section 3.5).

### To Be Done

- Deflections and shape distortions of the liquid jet as it enters the magnetic field should be estimated (and later calculated when the programs became available), and the interaction of the proton beam with this distorted shape simulated.
- Production with lead/tin should be calculated and the optimum angle, length and radius determined for this case.

## 2.3 Capture and matching Solenoids

The 20 T capture solenoid would be a hybrid, with copper (insert) and superconducting (outsert), magnet similar to that discussed in Feasibility Study 1. However, it is proposed here to use hollow copper conductor for the insert, rather than a Bitter style magnet in Study 1. The choice is aimed at achieving longer magnet life and avoiding any problems with highly irradiated water insulation. It is understood that the initial cost will be higher.

After the 20 T magnet, coils are designed to taper the axial field down slowly to 1.25 T over a distance of approximately 18 m. The form of the tapered field is approximately:

$$B(z) \approx \frac{20}{1 + k\, z}$$

Dimensions of coils that achieve this taper are given in the following table: The final design will have to include space for the beam dump and shielding.

| len1 | dl | rad | dr | | I/A |
|---|---|---|---|---|---|
| m | m | m | m | | A/mm$^2$ |
| 0.520 | 0.103 | 0.075 | 0.051 | 3 | 45.00 |
| 0.520 | 0.475 | 0.126 | 0.027 | 3 | 48.80 |
| 0.520 | 0.616 | 0.153 | 0.064 | 3 | 36.40 |
| 0.520 | 0.755 | 0.217 | 0.083 | 3 | 23.50 |
| 0.245 | 0.882 | 0.400 | 0.320 | 3 | 46.60 |
| 1.177 | 0.517 | 0.400 | 0.232 | 3 | 47.70 |
| 1.744 | 0.485 | 0.522 | 0.190 | 3 | 48.40 |
| 2.279 | 0.710 | 0.692 | 0.143 | 3 | 50.10 |
| 3.039 | 0.959 | 0.919 | 0.102 | 3 | 52.20 |
| 4.048 | 1.465 | 1.260 | 0.085 | 3 | 53.50 |
| 5.563 | 3.153 | 1.500 | 0.047 | 3 | 59.10 |
| 8.766 | 4.707 | 1.500 | 0.023 | 1 | 73.70 |
| 13.523 | 6.700 | 1.500 | 0.013 | 1 | 77.74 |
| 20.273 | 6.700 | 1.500 | 0.013 | 1 | 77.74 |

These coils, and their axial field profile, are shown in the following figures:

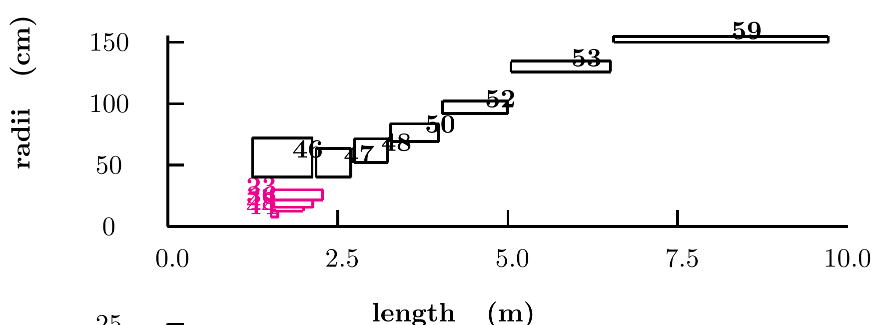


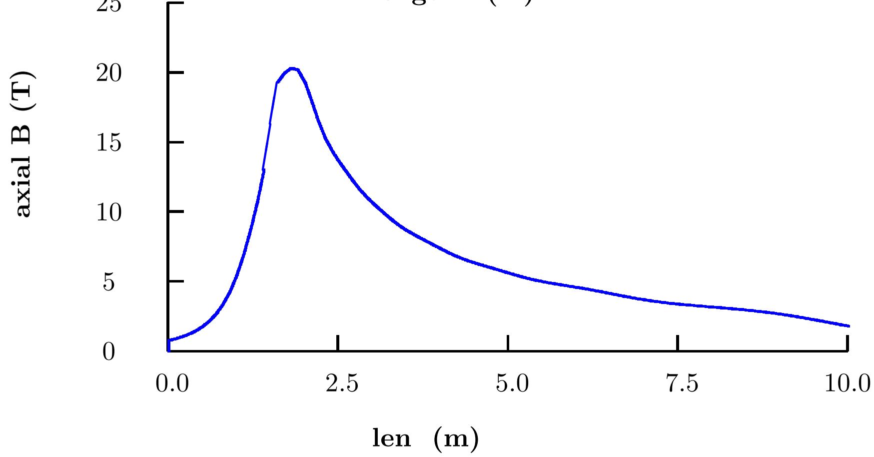

## To Be Done

- Design Beam dump and shielding, and modify coil designs to allow for them.

### 2.4 Drift 1

| | | |
|---|---|---|
| length | 18 | m |
| bore diameter | 60 | cm |
| axial field | 1.25 | T |

The real drift would be formed of spaced solenoids, and would have some finite periodicity. Design and simulation of this is yet to be done.

## To Be Done

- Design periodic focusing channel and simulate.

### 2.5 Induction Linac 1

| | | |
|---|---|---|
| length | 100 | m |
| inner radius | 30 | cm |
| Solenoid field | 1.25 | T |
| maximum gradient | 1.4 | MV/m |
| pulse length | 125 | nsec |

The real focusing magnetic field would be formed of spaced solenoids, and would have some finite periodicity (approx 1 m). Design and simulation of this is yet to be done.

The shape of the accelerating pulse is given in the following table and plot:

| time ns | Grad MV/m |
|---|---|
| 0 | -.06 |
| 10 | .29 |
| 25 | .66 |
| 45 | .94 |
| 85 | 1.23 |
| 125 | 1.39 |

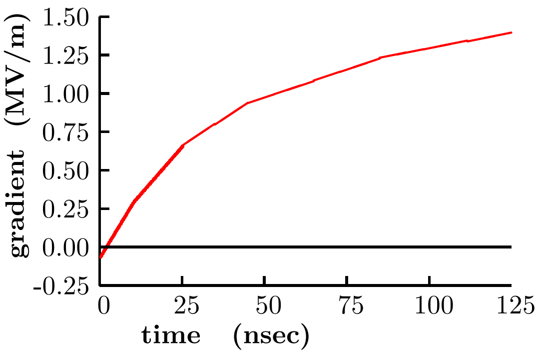


The total voltage gain is important, not the length or gradients used to achieve it.

## To Be Done

- Design periodic focusing channel and simulate.
- Optimize induction length and gradient for minimum cost.
- Consider if there is an advantage in using differing pulse shapes along the unit.

## 2.6 Mini-cooling and Field reversal

After a 3.25 m drift, there are two large hydrogen absorbers (1.75 m long each)

| | | |
|---|---|---|
| hydrogen length | $2 \times 1.75$ | m |
| hydrogen radius | 30 | cm |
| Solenoid fields | 1.25 | T |

Between the two hydrogen absorbers, there is a 10 m long chromatically matched field reversal. This reversal in needed for two reasons:

- between two halves of the absorber, it is needed to avoid generating finite canonical angular momentum from the reduction of angular momentum in the absorbers; and
- at some point along the phase rotation a field reversal is needed to avoid generating a correlation between the canonical angular momenta of individual tracks and their energy after correction by the induction units.

By serendipity, a single flip appears to meet both requirements.

The field reversal was designed to match $\beta$'s from start to end, over a momentum bite of 200 $+/-$ 90 MeV. The coils used in the optimization were larger than needed and had very low current densities. More reasonable coils will be relatively easy to design, but it has not yet been done. We thus specify the reversal by the required axial fields:

| length m | Field T |
|---|---|
| .000 | -1.25 |
| .2655 | -1.2446 |
| .5309 | -1.2242 |
| .7963 | -1.1874 |
| 1.0617 | -1.1357 |
| 1.3271 | -1.0852 |
| 1.5925 | -1.0664 |
| 1.8579 | -1.0801 |
| 2.1233 | -1.0661 |
| 2.3887 | -.97434 |
| 2.6541 | -.84339 |
| 2.9195 | -.76098 |
| 3.1849 | -.78458 |
| 3.4503 | -.9125 |
| 3.7157 | -1.0631 |
| 3.9811 | -1.0747 |
| 4.2465 | -.81469 |
| 4.5119 | -.30422 |
| 4.7773 | .30242 |

continued

| | |
|---|---|
| 5.0427 | .81346 |
| 5.3081 | 1.0744 |
| 5.5735 | 1.0635 |
| 5.8389 | .913 |
| 6.1043 | .78483 |
| 6.3697 | .76088 |
| 6.6351 | .84302 |
| 6.9005 | .97396 |
| 7.1659 | 1.0659 |
| 7.4313 | 1.0802 |
| 7.6967 | 1.0664 |
| 7.9621 | 1.0851 |
| 8.2275 | 1.1355 |
| 8.4929 | 1.1873 |
| 8.7583 | 1.2241 |
| 9.0237 | 1.2445 |
| 9.2891 | 1.251 |
| 10.0 | 1.25 |

These axial fields are plotted in the following figure, together with the $\beta$'s obtained for a set of different momenta.

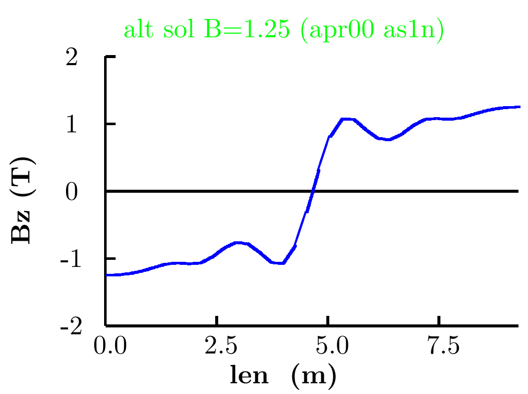


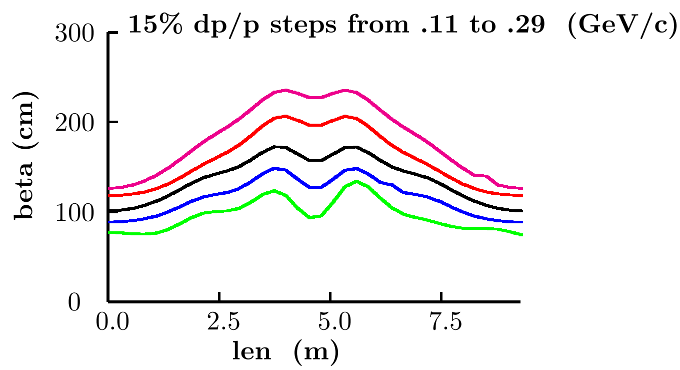

### To Be Done

- Design realistic coils to generate the required field.
- Determine thickness and shape of hydrogen windows and simulate their effects.

## 2.7 Drift 2

| | | |
|---|---|---|
| length | 123.25 | m |
| bore diameter | 60 | cm |
| axial field | 1.25 | T |

As for drift 1, the real drift would be formed of spaced solenoids, and would have some finite periodicity.

## 2.8 Induction Linac 2

| | | |
|---|---|---|
| length | 80 | m |
| inner radius | 30 | cm |
| Solenoid field | 1.25 | T |
| maximum gradients | -1.10 to +1.03 | MV/m |
| pulse length | 350 | nsec |

As for the first induction unit, the real focusing magnetic fields would be formed of spaced solenoids, and would have some finite periodicity (approx 1 m). Design and simulation of this is yet to be done.

The shape of the accelerating pulse is given in the following table and plot:

| time ns | Grad MV/m |
|---|---|
| 0 | -1.1 |
| 25 | -0.48 |
| 50 | 0.00 |
| 90 | 0.43 |
| 150 | 0.78 |
| 250 | 1.03 |
| 350 | 0.93 |

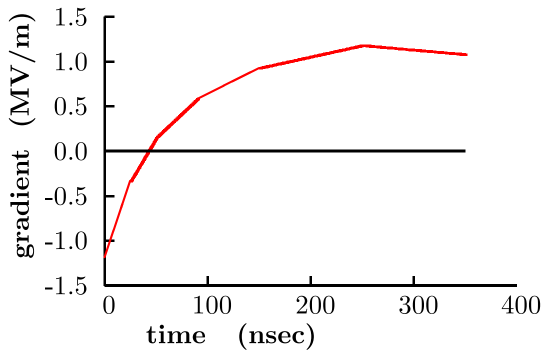


As in the first induction linac, the total voltage gain is important, not the length or gradients used to achieve it.

## To Be Done

- Design periodic focusing channel and simulate.

## 2.9 Match form solenoid to super FOFO lattice

A match is required between the approximately uniform 1.25 T solenoid fields in the previous sections, and the super FOFO lattices used in the following. This match should be chromatically matched, but since the momentum spread is relatively small ($\approx 4$ % rms), the chromatic correction is less critical than, for instance, in the field reversal.

The following table gives coil dimensions and current densities for the match. The current densities given here are lower than used in the following lattice and should be increased here too, to minimize their cost.

| len1 | dl | rad | dr | | I/A |
|---|---|---|---|---|---|
| m | m | m | m | | A/mm$^2$ |
| 0.000 | 1.375 | 0.300 | 0.100 | 2 | -9.99 |
| 1.375 | 1.375 | 0.300 | 0.100 | 2 | -9.99 |
| 2.750 | 1.375 | 0.300 | 0.100 | 2 | -9.99 |
| 4.125 | 1.375 | 0.300 | 0.100 | 2 | -9.99 |
| 5.500 | 1.375 | 0.300 | 0.100 | 2 | -9.99 |
| 6.875 | 1.375 | 0.300 | 0.100 | 2 | -9.99 |
| 8.250 | 0.330 | 0.300 | 0.110 | 2 | -15.57 |
| 8.949 | 0.187 | 0.330 | 0.330 | 6 | -33.40 |
| 9.466 | 0.187 | 0.330 | 0.330 | 6 | 35.19 |
| 10.511 | 0.330 | 0.770 | 0.110 | 2 | 66.12 |
| 11.665 | 0.187 | 0.330 | 0.330 | 6 | 43.75 |
| 12.182 | 0.187 | 0.330 | 0.330 | 6 | -43.75 |
| 13.227 | 0.330 | 0.770 | 0.110 | 2 | -67.40 |
| 14.415 | 0.187 | 0.330 | 0.330 | 6 | -43.75 |
| 14.932 | 0.187 | 0.330 | 0.330 | 6 | 43.75 |
| 15.977 | 0.330 | 0.770 | 0.110 | 2 | 66.12 |
| 17.165 | 0.187 | 0.330 | 0.330 | 6 | 43.75 |

The coils, their fields, and the $\beta$'s for three different momenta are plotted in the following figure:

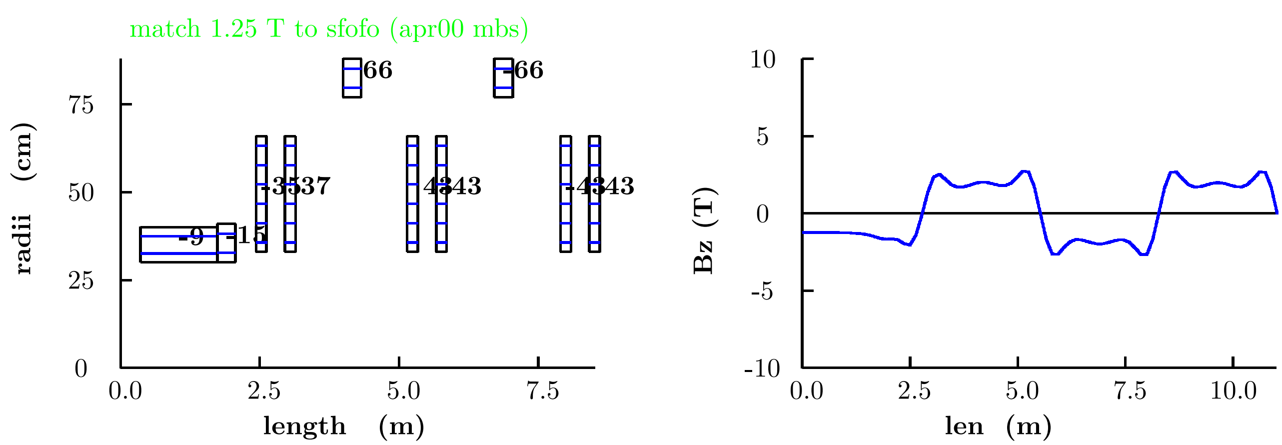

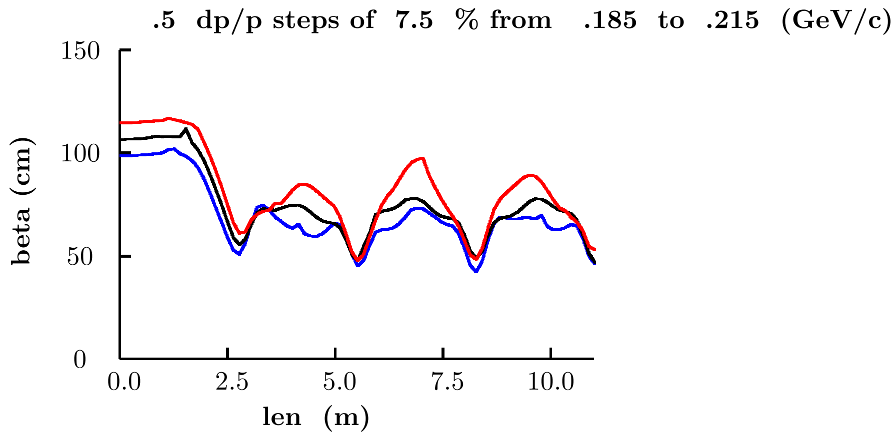


It is seen that the match is not very good, although there appear to be little adverse consequences.

The apertures in this matching section were set wide open and have not yet been optimized.

## To Be Done

- Improve the match design
- Use the higher current densities (suggested by John Miller) as used in the cooling sections.
- Determine the optimum apertures.

### 2.10 Buncher

The bunching is done in the same lattice as used for the first cooling stage (1,1), which is described in section 2.11. A total of 20 cells are used, giving it a length of $20 \times 2.75 = 55$ m.

The buncher consists of three stages:

1. low field 200 MHz rf with 400 MHz harmonic, followed by a long drift (27.5 m )
2. medium field 200 MHz rf with 400 MHz harmonic, followed by a shorter drift (11 m )
3. higher field 200 MHz rf followed by a short drift (5.5 m )

### 2.10.1 RF

The locations and lengths of the RF components are listed in the following table:

| | len<br>m | freq<br>MHz | grad<br>Mv/m |
|---|---|---|---|
| harmonic rf | .186 | 402.5 | 6.4 |
| space | .443 | | |
| rf | 4 × .373 | 201.25 | 6.4 |
| space | .443 | | |
| harmonic rf | .186 | 402.5 | 6.4 |
| drift 1 | 10 × 2.75 | | |
| harmonic rf | .186 | 402.5 | 6 |
| space | .443 | | |
| rf | 4 × .373 | 201.25 | 6 |
| space | .443 | | |
| harmonic rf | 2 × .186 | 402.5 | 6 |
| space | .443 | | |
| rf | 4 × .373 | 201.25 | 6 |
| space | .443 | | |
| harmonic rf | .186 | 402.5 | 6 |
| drift 2 | 3 × 2.75 | | |
| space | .629 | | |
| rf | 4 × .373 | 201.25 | 8 |
| space | .629 | | |
| space | .629 | | |
| rf | 4 × .373 | 201.25 | 8 |
| space | .629 | | |
| drift 3 | 2 × 2.75 | | |

### 2.10.2 RF window radii and thicknesses

| | rad<br>m | thickness<br>$\mu$m |
|---|---|---|
| windows at ends of each 400 MHz cavity | .2 | 100 |
| windows at end of each set of 4 200 MHz cavities | .21 | 125 |
| windows between the 4 400 MHz cavities | .25 | 250 |

## To Be Done

- Determine the required window thicknesses and simulate.
- Design the cavities and simulate.

- Find if there is sufficient space inside the smaller coils for the harmonic RF, and redesign the lattice with larger inside radii, if needed.

## 2.11 Cooling Latices

### 2.11.1 Introduction

The cooling is done in six sections with steadily decreasing $\beta$'s. This is done to maximize the cooling rate. Too small a $\beta$ at a given emittance results in too large divergence angles and particle loss. Too large a $\beta$ gives small divergence angles and a greater relative emittance growth from coulomb scattering. The best $\beta$ scales down with the emittance and is always such as to give a certain constant divergence angles ($\sigma_{x'} = \sigma_{y'} \approx 0.1$).

The six sections are made from two different physical lattices [(1) and (2)], with three different current setting in each: 1,1 1,2 1,3 in the first lattice, and 2,1 2,2 2,3, in the second. The final cooling section (2,3) is further broken into 2 parts (2,3a) and (2,3b) that differ only in their window sizes and thicknesses.

The lengths of the sections are:

| | length<br>m | from target<br>m |
|---|---|---|
| cool 1,1 | $6 \times 2.75 = 16.5$ | 444.9 |
| cool 1,2 | $6 \times 2.75 = 16.5$ | 461.4 |
| cool 1,3 | $6 \times 2.75 = 16.5$ | 477.9 |
| cool 2,1 | $14 \times 1.65 = 23.1$ | 501 |
| cool 2,2 | $10 \times 1.65 = 16.5$ | 517.5 |
| cool 2,3a | $16 \times 1.65 = 26.4$ | 543.9 |
| cool 2,3b | $16 \times 1.65 = 26.4$ | 570.3 |

The lattices used have been named "Super FOFO". The "FOFO" refers to the basic sequence of alternating solenoids, that focus the beam and generate $\beta$, and thus beam size, minima between the solenoids. The "Super" part, proposed by A. Sessler, is the replacement of the simple alternating solenoids with alternating, but more complex, solenoid systems. In this case the systems consist of strong short "focusing" solenoids at either end, and a weaker "coupling" fields between them.

An example of the fields (for the last part) is given below

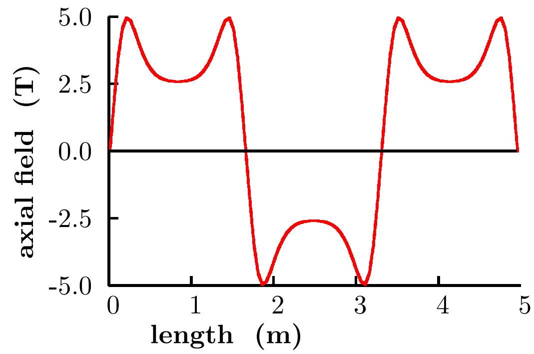


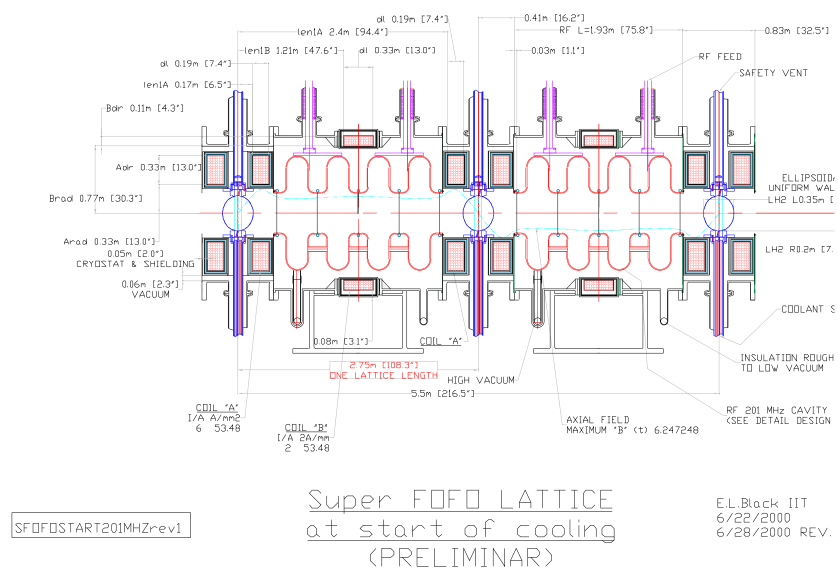


The following figure shows the beta's, as a function of momentum, for the six cases.

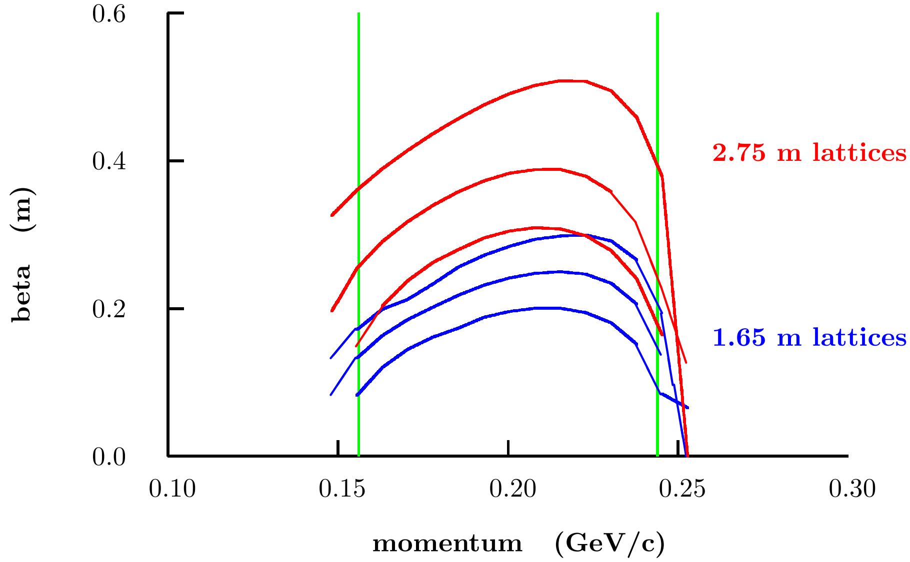


In all cases the $\beta$ functions are seen to have sharp drops above and below the required momentum acceptance. These are due to the approach to two resonances. At the lower momentum it corresponds to a 2 $\pi$ phase advance per cell, and at the higher momentum to 1 $\pi$ phase advance. With any given lattice length, the central beta and its location can be controlled by adjusting two characteristics, or parameters, of the focusing fields. The details of the fields are not important, just these two characteristics:

- the strength of the opposed "focusing" fields near the lattice ends (the higher the fields, the higher the momentums focused)
- the general magnitude of the field in the central part of the lattice (a higher "coupling" field reduces the end betas, but increases the momentum acceptance)

By adjusting these two characteristics, we can keep the betas symmetric about the required mean momentum, and independently reduce the central beta value. But as we decrease the coupling fields, the momentum acceptance shrinks and, at some point, becomes unacceptably small. At this point we are forced to use a shorter lattice which, though it will require higher fields, allows the betas to be further reduced while again achieving adequate momentum acceptance and keeping the betas symmetric.

The two characteristics can be obtained in a number of different ways. The required lattice performance can, for instance, be obtained by having only a pair of oppositely driven short solenoids on either side of each absorber. The two parameters to be controlled, in this case, are the currents and locations of the coils. However, in this case, the space for RF between the "focusing" coils is limited.

Another method is to use pancake shaped focus coils. The two parameters are the currents and outer radii of these pancacakes. Adequate space for the RF can be obtained and there is the added advantage that the RF has no coils outside it. But the peak fields in this design are higher, and the ampere turns much higher (up to a factor of 3).

The chosen solution is thus to use a separate "coupling" coil outside the RF, and power it independently of the "focusing" coils at the ends. This arrangement has the big advantage that the two parameters are just the two currents, and the betas can be varied, and the symmetry maintained, by adjusting these currents without changing the physical design. This done here, first with a 2.75 m long lattice, and then with a 1.65 m one. Three different sets of currents have been specified for each of the lattices, giving a total of six different central $\beta$'s. If desired, the number of different currents could be further increased to make the change of parameters even more adiabatic, but this will not change the physical designs.

Specific coil dimensions, current densities and fields they generate are given below, but it should be understood that the exact shape of the fields is not important provided that the approximate locations and magnitudes of the end fields, and the approximate magnitude of the central fields are achieved.

The axial fields along the full cooling channel are shown below. The field and periodicity changes can clearly be seen.

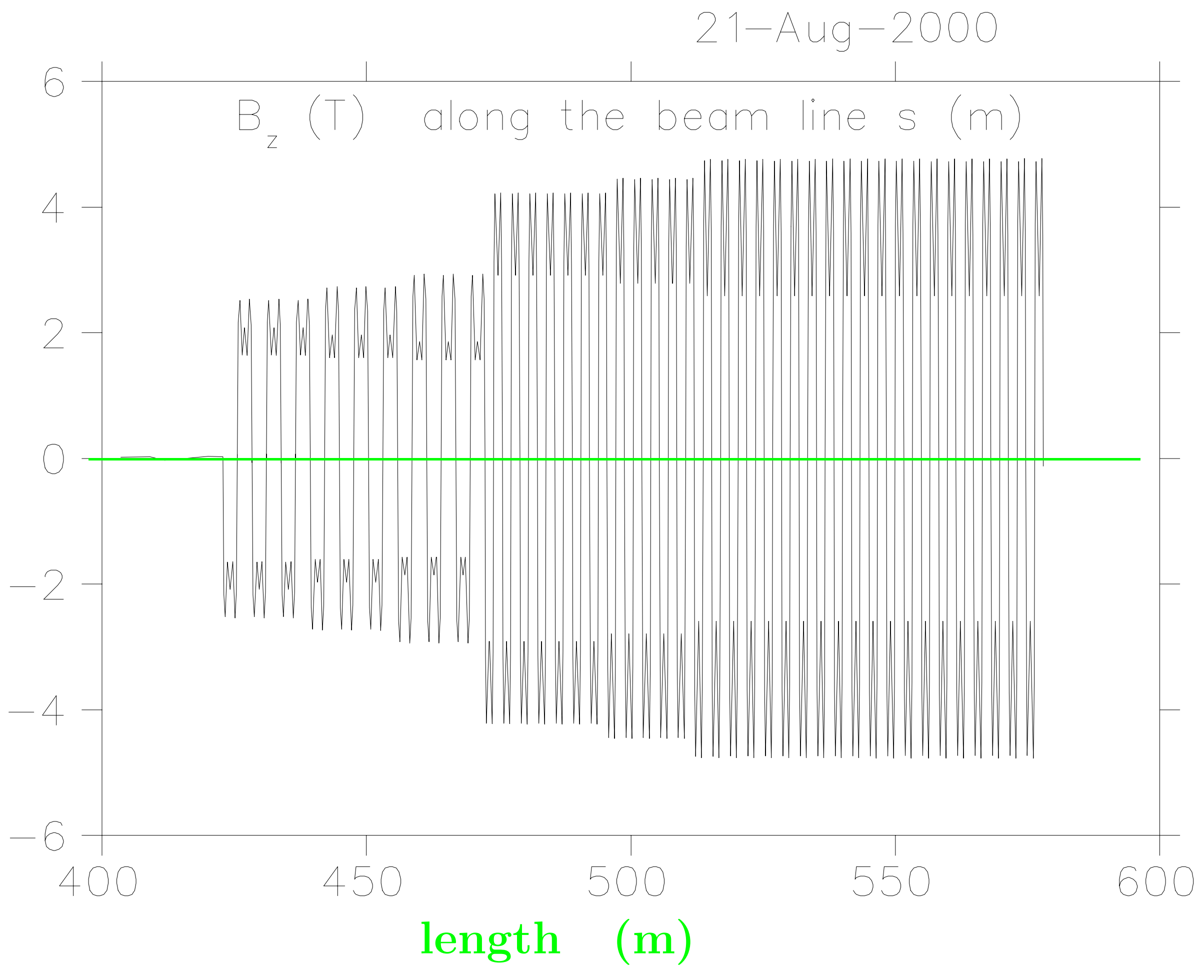


**$B_z$ fields along the beam line (T)**

#### 2.11.2 Coil dimensions and fields

The physical coil dimensions and the three different current setting, for the first (2.75 m long) lattice, are:

| len1 | dl | rad | dr | j(1,1) | j(1,2) | j(1,3) |
|---|---|---|---|---|---|---|
| m | m | m | m | | A/mm$^2$ | |
| 0.175 | 0.167 | 0.330 | 0.175 | 75.96 | 84.17 | 92.39 |
| 1.210 | 0.330 | 0.770 | 0.080 | 99.24 | 92.42 | 85.61 |
| 2.408 | 0.167 | 0.330 | 0.175 | 75.96 | 84.17 | 92.39 |

The fields are:

continued

| | 1,1 | 1,2 | 1,3 |
|---|---|---|---|
| 0 | 0 | 0 | 0 |
| .05 | .6697 | .737 | .8032 |
| .1 | 1.325 | 1.456 | 1.584 |
| .15 | 1.903 | 2.088 | 2.269 |
| .2 | 2.36 | 2.587 | 2.808 |
| .25 | 2.667 | 2.918 | 3.163 |
| .3 | 2.81 | 3.067 | 3.32 |
| .35 | 2.802 | 3.05 | 3.293 |
| .4 | 2.682 | 2.906 | 3.129 |
| .45 | 2.496 | 2.689 | 2.882 |
| .5 | 2.287 | 2.446 | 2.606 |
| .55 | 2.088 | 2.213 | 2.34 |
| .6 | 1.918 | 2.012 | 2.107 |
| .65 | 1.785 | 1.85 | 1.917 |
| .7 | 1.692 | 1.732 | 1.773 |
| .75 | 1.635 | 1.652 | 1.671 |
| .8 | 1.61 | 1.608 | 1.607 |
| .85 | 1.613 | 1.593 | 1.574 |
| .9 | 1.638 | 1.603 | 1.567 |
| .95 | 1.68 | 1.631 | 1.581 |
| 1 | 1.735 | 1.673 | 1.611 |
| 1.05 | 1.797 | 1.723 | 1.65 |
| 1.1 | 1.862 | 1.778 | 1.694 |
| 1.15 | 1.925 | 1.832 | 1.74 |
| 1.2 | 1.981 | 1.882 | 1.782 |
| 1.25 | 2.028 | 1.922 | 1.817 |
| 1.3 | 2.06 | 1.951 | 1.842 |
| 1.35 | 2.077 | 1.966 | 1.855 |
| 1.4 | 2.077 | 1.966 | 1.855 |
| 1.45 | 2.06 | 1.951 | 1.842 |
| 1.5 | 2.028 | 1.922 | 1.817 |
| 1.55 | 1.981 | 1.882 | 1.782 |
| 1.6 | 1.925 | 1.832 | 1.74 |
| 1.65 | 1.862 | 1.778 | 1.694 |
| 1.7 | 1.797 | 1.723 | 1.65 |
| 1.75 | 1.735 | 1.673 | 1.611 |
| 1.8 | 1.68 | 1.631 | 1.581 |
| 1.85 | 1.638 | 1.603 | 1.567 |
| 1.9 | 1.613 | 1.593 | 1.574 |
| 1.95 | 1.61 | 1.608 | 1.607 |
| 2 | 1.635 | 1.652 | 1.671 |
| 2.05 | 1.692 | 1.732 | 1.773 |
| 2.1 | 1.785 | 1.85 | 1.917 |
| 2.15 | 1.918 | 2.012 | 2.107 |
| 2.2 | 2.088 | 2.213 | 2.34 |
| 2.25 | 2.287 | 2.446 | 2.606 |
| 2.3 | 2.496 | 2.689 | 2.882 |
| 2.35 | 2.682 | 2.906 | 3.129 |
| 2.4 | 2.802 | 3.05 | 3.293 |
| 2.45 | 2.812 | 3.07 | 3.322 |
| 2.5 | 2.669 | 2.92 | 3.166 |
| 2.55 | 2.362 | 2.589 | 2.81 |
| 2.6 | 1.903 | 2.088 | 2.27 |
| 2.65 | 1.325 | 1.456 | 1.584 |
| 2.7 | .6697 | .737 | .8032 |
| 2.75 | 0 | 0 | 0 |

The coils and axial fields are shown below. The maximum field at the coils occurs in case 1,3, and is 7.4 T.

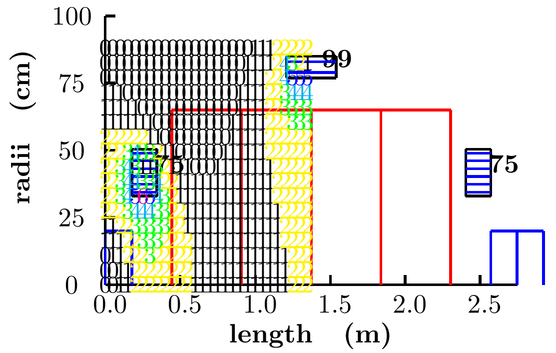


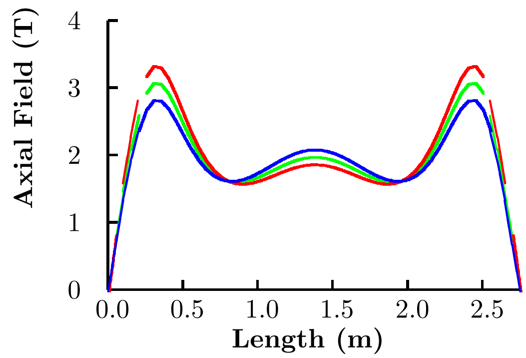


The beta functions in lattice (1,3), for a number of momenta, as a function of position along the cell are:

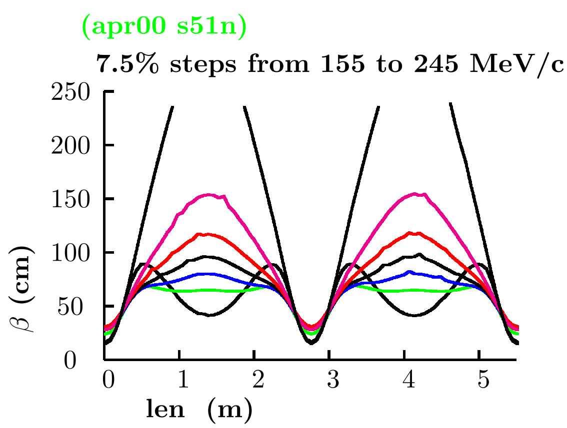


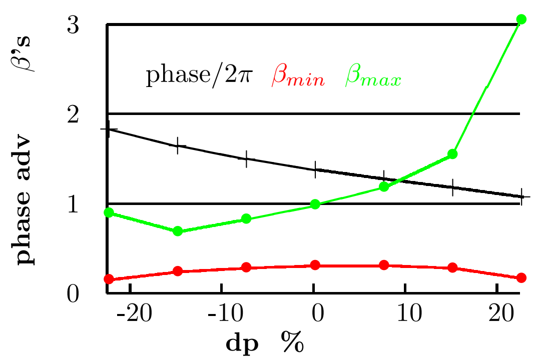

And for the second (1.65 m long) lattice, the coils are:

| len1 | dl | rad | dr | j(2,1) | j(2,2) | j(2,3) |
|---|---|---|---|---|---|---|
| m | m | m | m | | A/mm$^2$ | |
| 0.066 | 0.145 | 0.198 | 0.330 | 71.63 | 78.14 | 86.82 |
| 0.627 | 0.396 | 0.792 | 0.099 | 99.48 | 91.52 | 79.58 |
| 1.439 | 0.145 | 0.198 | 0.330 | 71.63 | 78.14 | 86.82 |

The fields are given in the following table

| | 2,1 | 2,2 | 2,3 |
|---|---|---|---|
| 0 | 0 | 0 | 0 |
| .05 | 1.552 | 1.678 | 1.845 |
| .1 | 2.976 | 3.2 | 3.495 |
| .15 | 3.91 | 4.187 | 4.551 |
| .2 | 4.307 | 4.588 | 4.955 |
| .25 | 4.283 | 4.531 | 4.85 |
| .3 | 4.035 | 4.228 | 4.473 |
| .35 | 3.725 | 3.859 | 4.023 |
| .4 | 3.447 | 3.525 | 3.611 |
| .45 | 3.232 | 3.262 | 3.281 |
| .5 | 3.084 | 3.072 | 3.034 |
| .55 | 2.991 | 2.946 | 2.86 |
| .6 | 2.94 | 2.867 | 2.744 |
| .65 | 2.917 | 2.823 | 2.67 |
| .7 | 2.91 | 2.801 | 2.626 |
| .75 | 2.91 | 2.791 | 2.601 |
| .8 | 2.912 | 2.787 | 2.591 |
| .85 | 2.912 | 2.787 | 2.591 |
| .9 | 2.91 | 2.791 | 2.601 |
| .95 | 2.91 | 2.801 | 2.626 |
| 1 | 2.917 | 2.823 | 2.67 |
| 1.05 | 2.94 | 2.867 | 2.744 |
| 1.1 | 2.991 | 2.946 | 2.86 |
| 1.15 | 3.084 | 3.072 | 3.034 |
| 1.2 | 3.232 | 3.262 | 3.281 |
| 1.25 | 3.447 | 3.525 | 3.611 |
| 1.3 | 3.725 | 3.859 | 4.023 |
| 1.35 | 4.035 | 4.228 | 4.473 |
| 1.4 | 4.283 | 4.531 | 4.85 |
| 1.45 | 4.307 | 4.588 | 4.955 |
| 1.5 | 3.91 | 4.187 | 4.551 |
| 1.55 | 2.976 | 3.2 | 3.495 |
| 1.6 | 1.552 | 1.678 | 1.845 |
| 1.65 | 0 | 0 | 0 |

and the coils and axial fields are plotted. The maximum field at the coils occurs in case 1,3, and is 8.5 T.

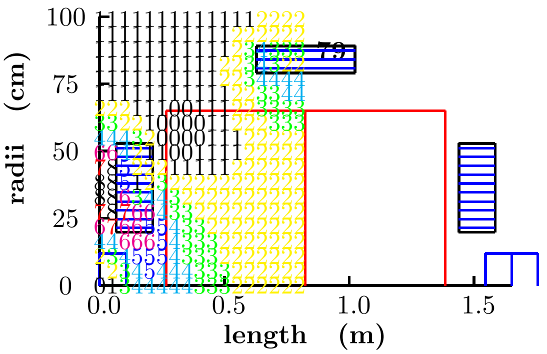


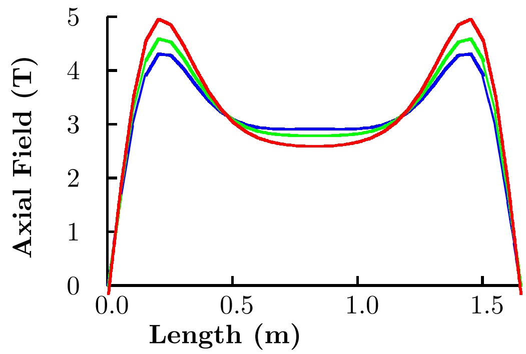


And the beta functions for (2,3):

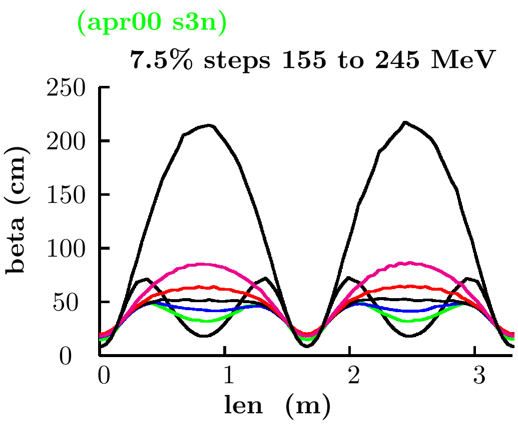


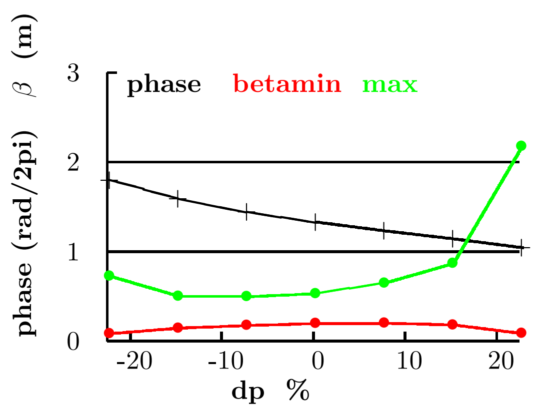


## To Be Done

- Try designing a third lattice with shorter cell, higher fields and yet lower beta, to further reduce the emittance. Determine the practicability of such a lattice and what cost savings in the following acceleration would be gained from the lower emittance achieved. The relevance of this will be significant only if emittance exchange can be used to decrease the particle loss with further cooling.

## 2.12 Cooling RF and absorbers

### 2.12.1 Absorbers and RF

The hydrogen absorbers and rf within the three 2.75 m lattices are all the same except for their apertures which will be given in a separate table.

| | dl<br>cm | gradient<br>MV/m |
|---|---|---|
| Hydrogen | 35/2 | |
| Space | 26.7 | |
| RF | 4 × 46.6 | 16.29 |
| Space | 26.7 | |
| Hydrogen | 35/2 | |

The hydrogen absorber and rf within the 1.65 m lattices are:

| | dl<br>cm | gradient<br>MV/m |
|---|---|---|
| Hydrogen | 21/2 | |
| Space | 16 | |
| RF | 2 × 55.9 | 17.6 |
| Space | 16 | |
| Hydrogen | 21/2 | |

### 2.12.2 Hydrogen window sizes and thicknesses

Material: Aluminum

| | rad<br>m | thickness<br>$\mu$m |
|---|---|---|
| 1.1 | .18 | 200 |
| 1.2 | .15 | 250 |
| 1.3 | .13 | 130 |
| 2.1 | .11 | 110 |
| 2.2 | .10 | 100 |
| 2.3a | .09 | 90 |
| 2.3b | .08 | 80 |

### 2.12.3 RF window sizes and thicknesses

Material: Beryllium

| | ends | | center | |
|---|---|---|---|---|
| | rad<br>m | thickness<br>$\mu$m | rad<br>m | thickness<br>$\mu$m |
| 1.1 | .25 | 250 | .21 | 125 |
| 1.2 | .25 | 250 | .21 | 125 |
| 1.3 | .25 | 250 | .21 | 125 |
| 2.1 | .21 | 125 | .18 | 75 |
| 2.2 | .18 | 75 | .18 | 75 |
| 2.3a | .18 | 75 | .15 | 75 |
| 2.3b | .15 | 50 | .15 | 50 |

## To Be Done

- Determine the required hydrogen and RF window thicknesses and re-simulate.
- Determine the hydrogen window thicknesses if they were made of AlBemet, and simulate.
- study the effects of windows with tapered thicknesses.
- Design rf cavities and simulate with the resulting fields.
- Study effects of random errors and set tolerances.
- Study effects of wake fields and space charge.
- Study the effects of differing theoretical assumptions about large angle scatters.

## 2.13 Acceleration

The requirements for the acceleration system are:

| | | |
|---|---|---|
| initial momentum | 210 | MeV/c |
| final energy | 20 | GeV |
| Transverse acceptance | 15 | mm rad |
| Longitudinal acceptance | 150 | mm |
| bunch spacing | 201.25 | MHz |
| number of bunches | 67 | |
| total muons per bunch train | 3 | $10^{13}$ |

The number of muons specified correspond to a 1.5 MW driver and 0.2 $\mu$'s/p.

# 3 Simulated Performance

## 3.1 Introduction

The front-end described above has been simulated using MARS to calculate pion production in the target, and ICOOL (version 2.07) to follow particles through the phase rotation and cooling. The runs used started with 5000 initial pions, yielding of the order 2000 final muons with statistical errors of approximately 3 %.

## 3.2 Phase Rotation

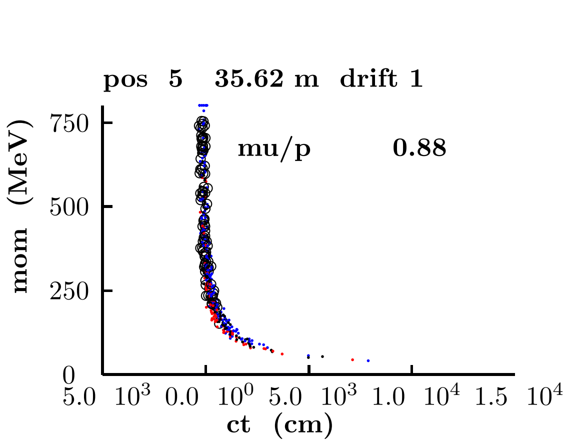


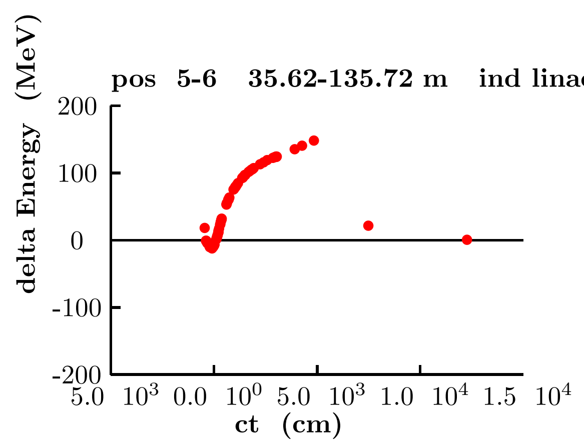


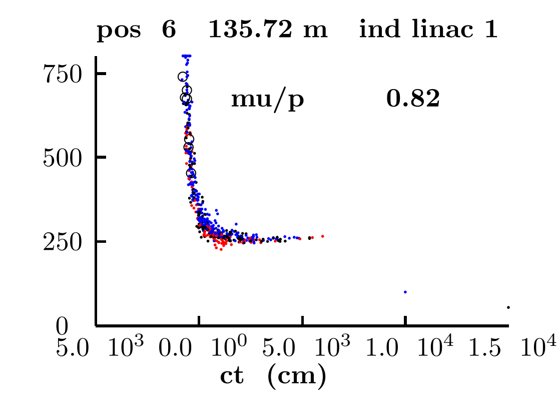


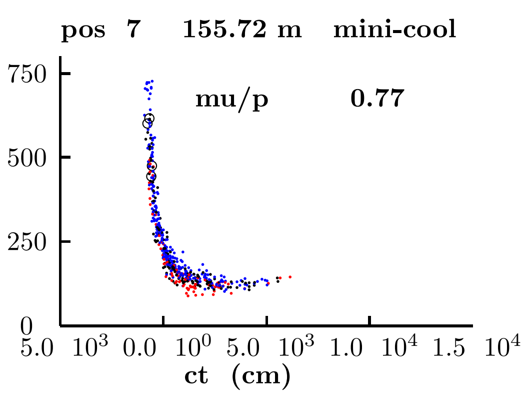

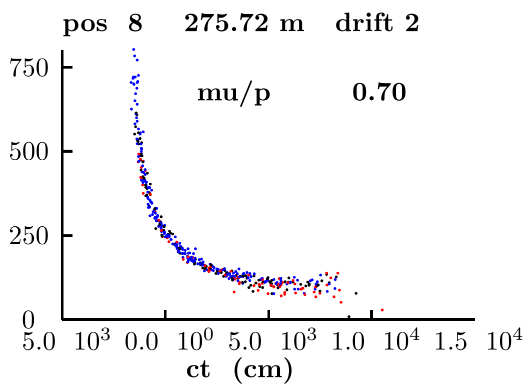
pos 8 275.72 m drift 2
mu/p 0.70
750
500
250
0
5.0 10^3 0.0 10^0 5.0 10^3 1.0 10^4 1.5 10^4
ct (cm)

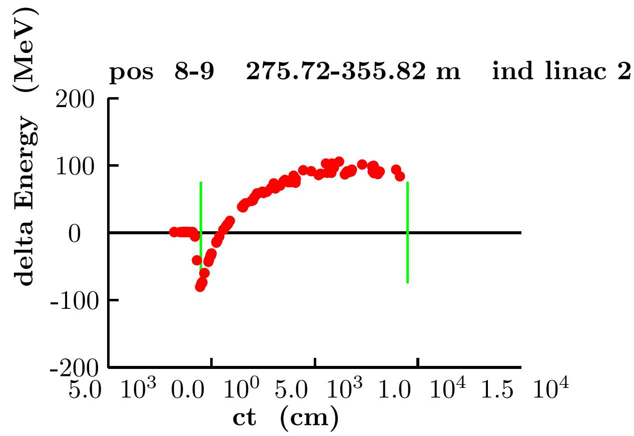
pos 8-9 275.72-355.82 m ind linac 2
delta Energy (MeV)
200
100
0
-100
-200
5.0 10^3 0.0 10^0 5.0 10^3 1.0 10^4 1.5 10^4
ct (cm)

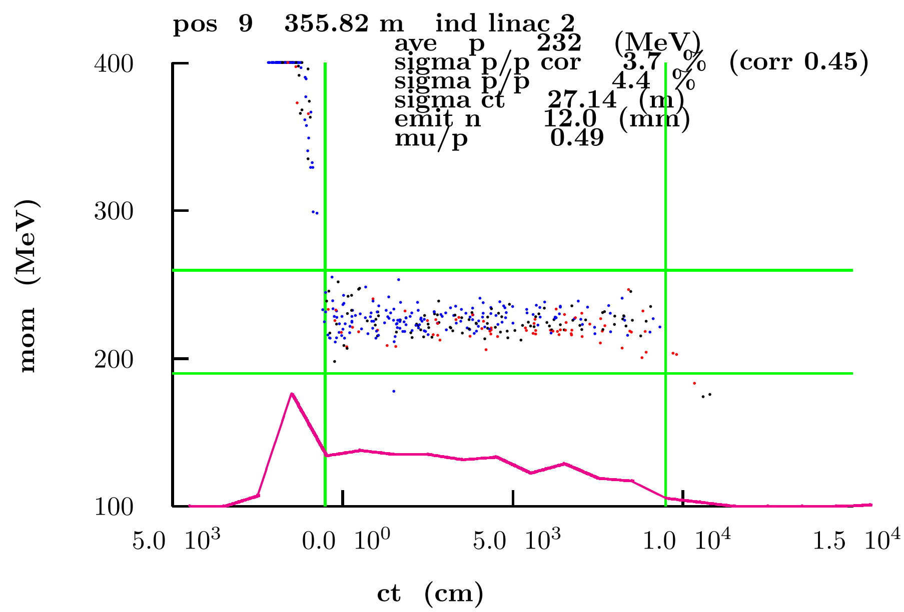
pos 9 355.82 m ind linac 2
ave p 232 (MeV)
sigma p/p cor 3.7 % (corr 0.45)
sigma p/p 4.4 %
sigma ct 27.14 (m)
emit n 12.0 (mm)
mu/p 0.49
mom (MeV)
400
300
200
100
5.0 10^3 0.0 10^0 5.0 10^3 1.0 10^4 1.5 10^4
ct (cm)

### 3.2.1 Correlations

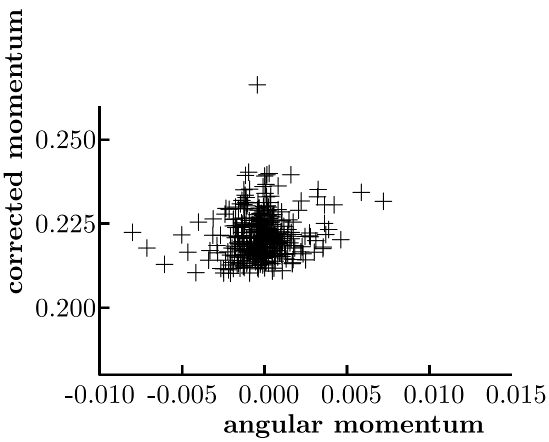


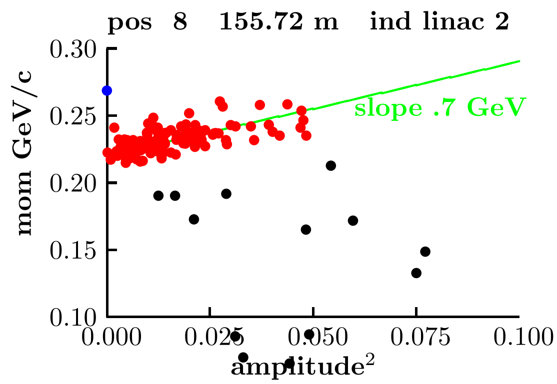


There is little correlation between momentum and angular momentum correlation, indicating that the field reversal is correctly located.

The momentum-amplitude correlation is seen to be 0.7. A higher value than without the mini cool (.45). Ideally the correlation should be such that forward velocity in the following lattice is independent of amplitude. A value of approximately 1.1 would be required for this, so further work to increase the correlation could be beneficial.

### 3.2.2 polarization

The calculated polarization as a function of bunch position at the end of the phase rotation, but before cooling, is shown below. In this calculation, spin tracking was not used:

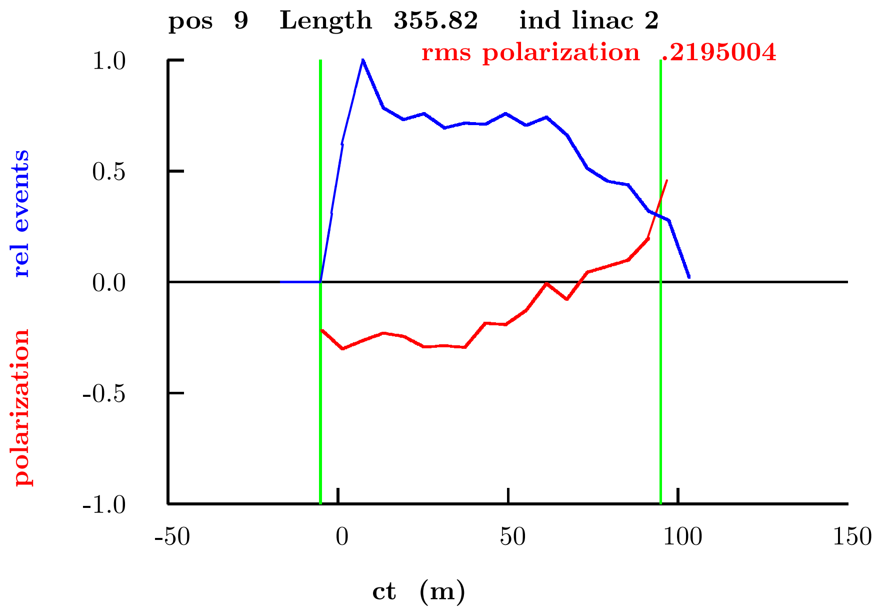


It is seen that although the polarization is less than in systems with RF close to the target (effective polarization ≈ .35 %), it is not negligible. To Be Done

- use spin tracking and material effects to determine polarization at end of front end.

#### 3.2.3 Phase Rotation Efficiency

The following figure show the distributions of initial pion energies for (black) all pions exiting the target and (blue) those pions that decayed to muons exiting the phase rotation. The following figure gives the ratios of these two and indicates that as many as 80 % of the lower energy pions yield muons at the end, with this efficency falling for higher energy pions that are made with higher transverse momenta and are more often lost in the initial capture and taper.

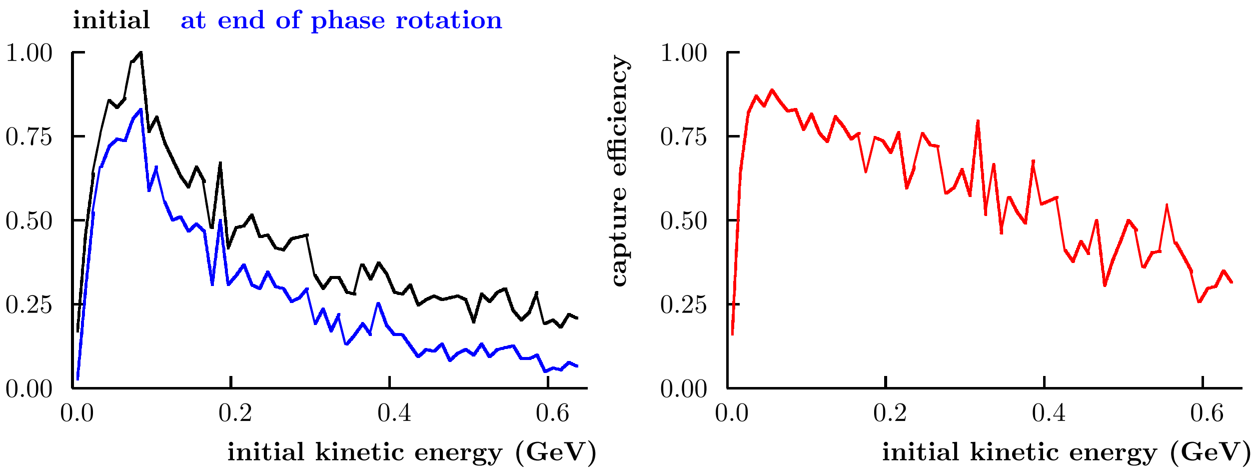


## 3.3 Buncher

The following figure shows the momentum-time distributions at the start, and after each of the three buncher phases. Distributions are also shown at the ends of the first and second cooling stages.In the last three distributions, ellipses are drawn indicating the approximate acceptance of the cooling channel.

It can be seen that at the end of the buncher, most, but not all, particles are within the approximately elliptical bucket. About 25 % are outside the bucket and are lost relatively rapidly, and another 25 % are lost more slowly as the longitudinal emittance rises from straggling and the negative slope of the energy loss with energy.

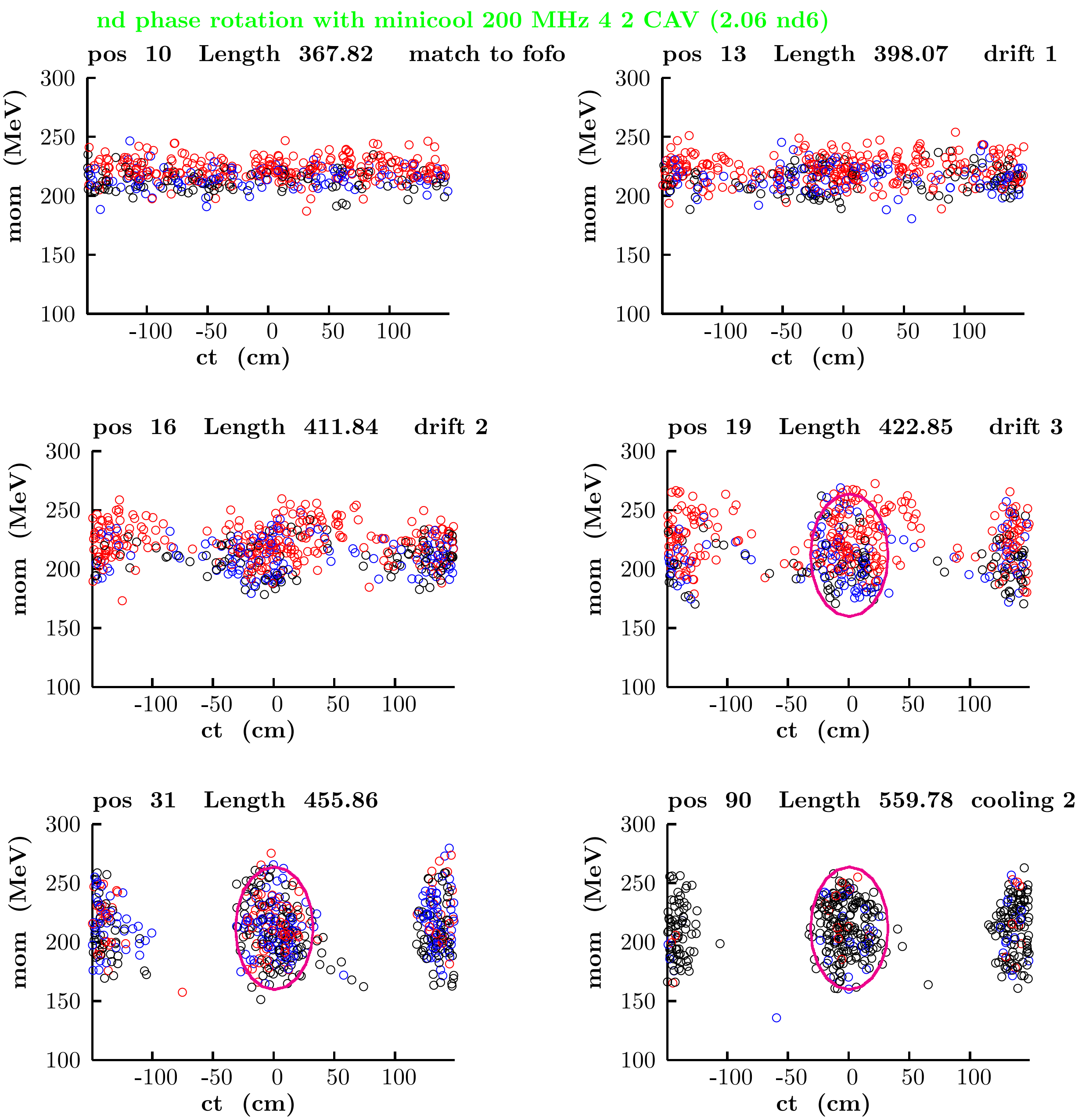


## 3.4 Cooling

In the following figure we see the beta functions and radii stepping down with each new cooling lattice, but the rms angular size remaining substantially constant:

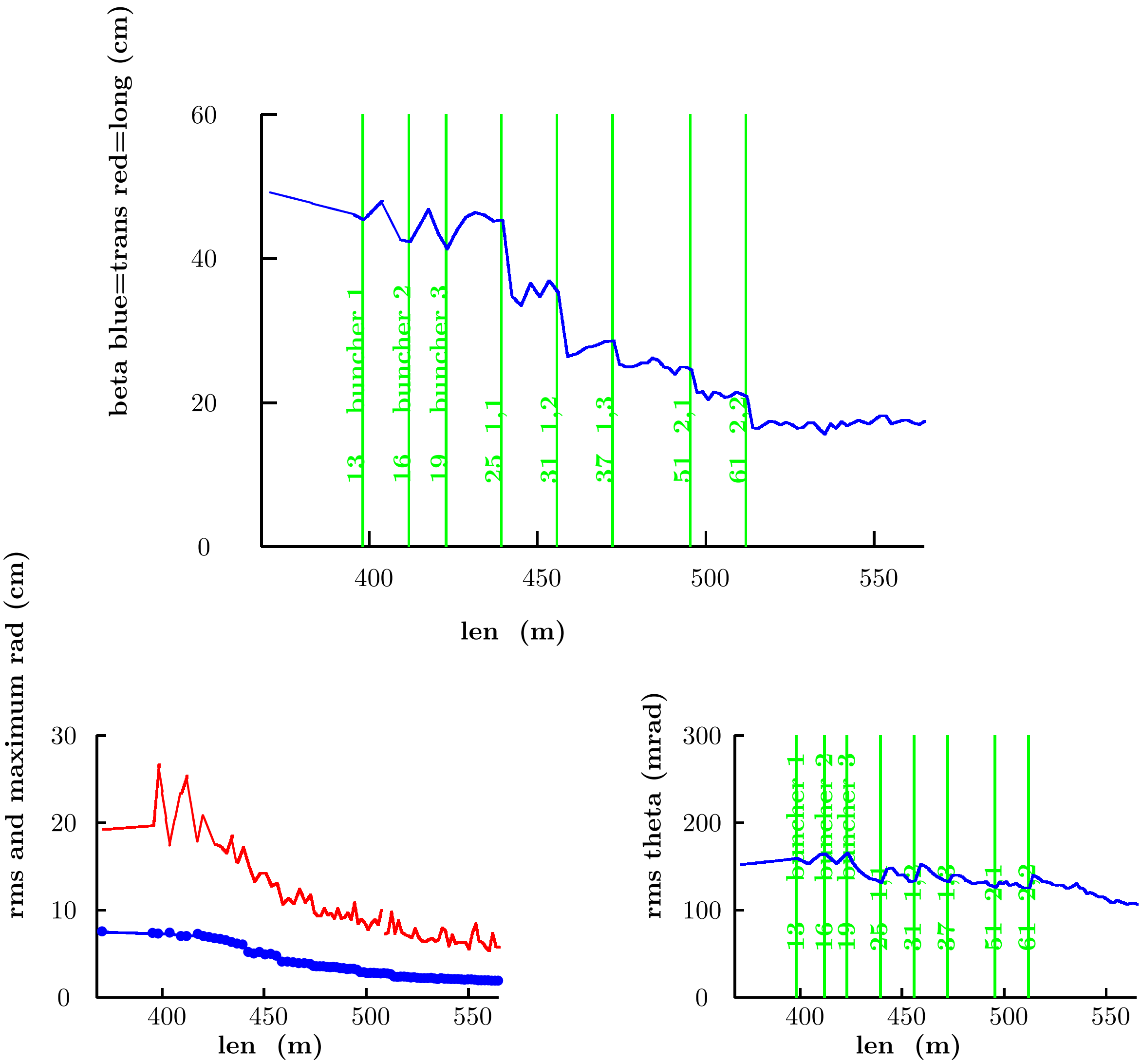


The transverse and longitudinal emittances through the cooling system are plotted below. They were calculated using Greg Penn's program and are diagonalize, i.e. they represent values corrected for correlations between the variables, including the strong momentum amplitude correlation.

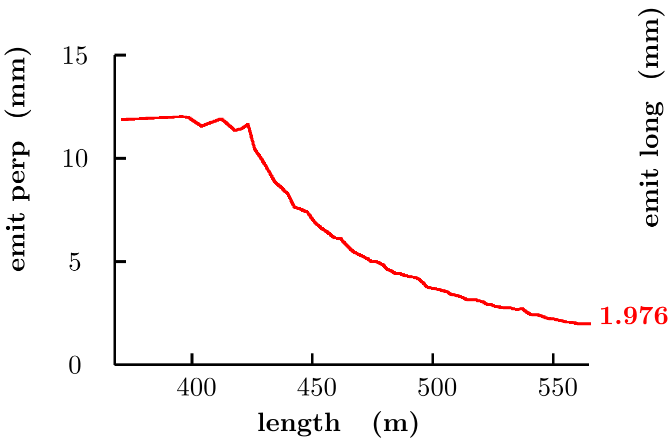


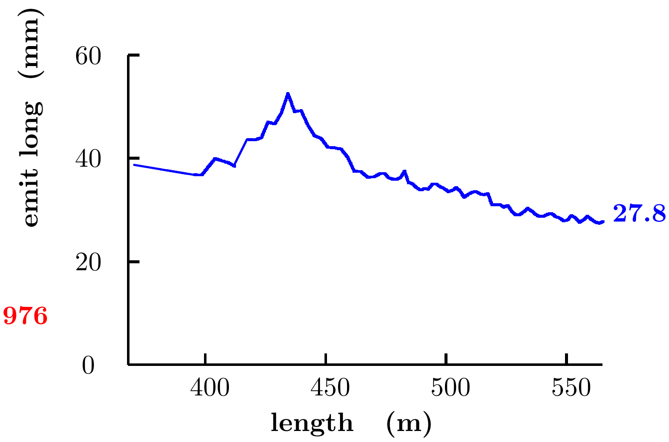


The transverse emittance is seen to cool from 12 to 2 mm radians. The longitudinal emittance shows an initial rise as particles not within the RF bucket are lost, and then an approach to an asymptotic value set by this bucket size. Naturally, this longitudinal emittance should rise due to straggling and the negative slope of energy loss with energy. But since the bucket is already full, the growth is reflected in a steady loss of particles as seen in the next plot. Despite this loss, the numbers of particles within the accelerator acceptances increases. The red and blue lines give the number of particles within these longitudinal and transverse acceptances. The red line represents the values for the accelerator parameters in this study. The blue line, given for comparison, gives the values for the acceptances used in the Feasibility Study 1.

- Longitudinal: $(dz^2/\beta_s \ + \ dp/p^2 \ \beta_s \ < \ 150$ (mm)
- Transverse (red): $(x^2+y^2)/\beta \ + \ (x'^2+y'^2)\beta \ < \ 15$ (mm rad)
- Transverse (blue): $(x^2+y^2)/\beta \ + \ (x'^2+y'^2)\beta \ < \ 9.75$ (mm rad)

where $\beta_s$ is the synchrotron beta ($\beta_s = \sigma_{dz}/\sigma_{dp/p}$), and $\beta$ is the transverse $\beta$.

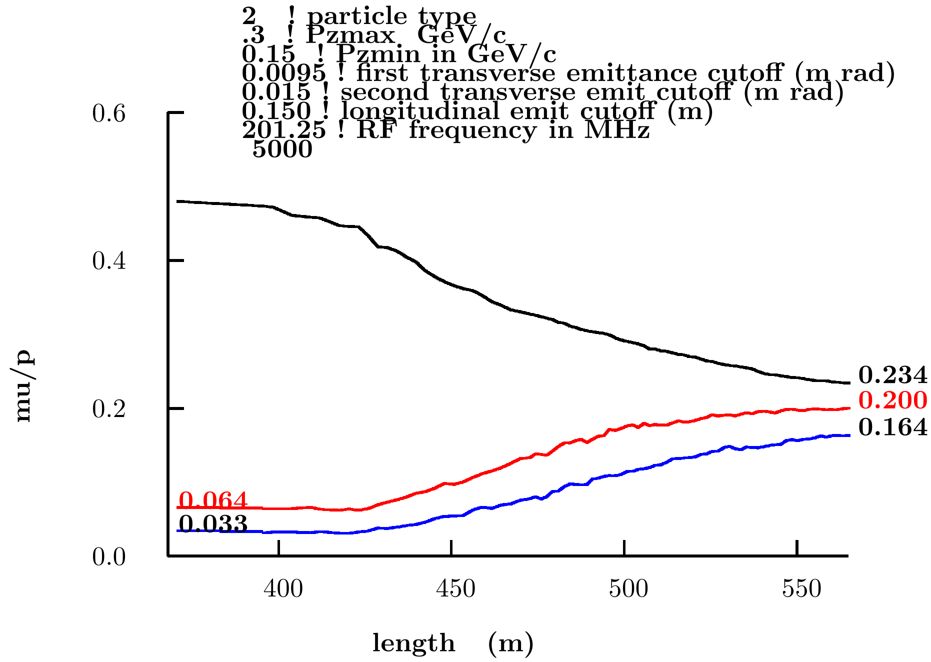


It is seen that the cooling's gain in muons within the acceptance is 3.1 $\times$, or 5 $\times$ if the study 1 acceptances were used. If the particle loss from longitudinal emittance growth could be eliminated, as should be the case with emittance exchange, then these gains would double.

### 3.4.1 Overall performance and efficiency

The transverse emittance along the entire front-end is plotted below:

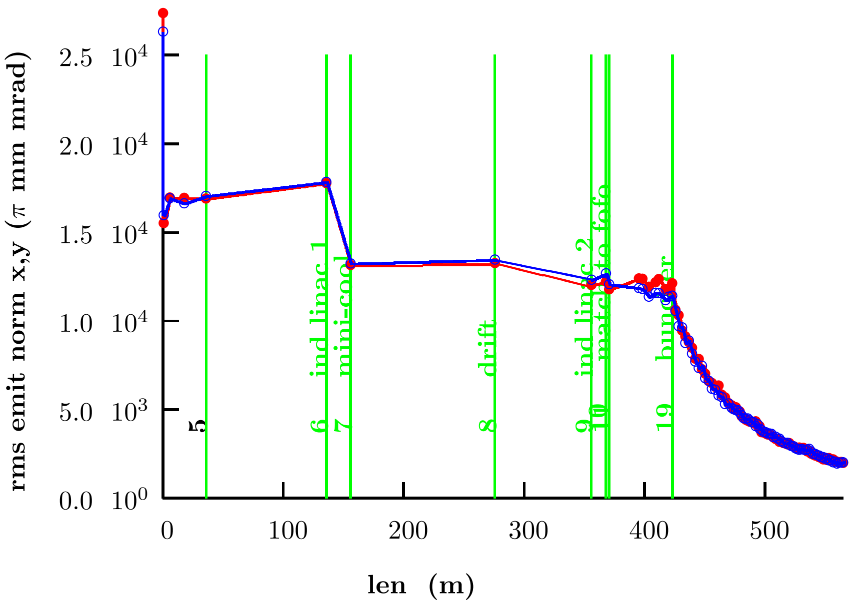


The emittance is seen to be reduced in the mini cooling at 150 m (from 18 to 13 mm rad), falls a little more as large amplitude particles are lost in the induction linac, and falls fast in the final cooling (from 12 to 2 mm rad).

The muons per proton along the full system are given below. The particle losses prior to the buncher come primarily from the loss of very high and very low momenta (about 30 %, plus some loss from muon decay (approx 20 %). The losses in the cooling come (≈25%) from bunching inefficiency and (≈25$) from loss of particles from the RF bucket as the longitudinal emittance grows in the cooling.

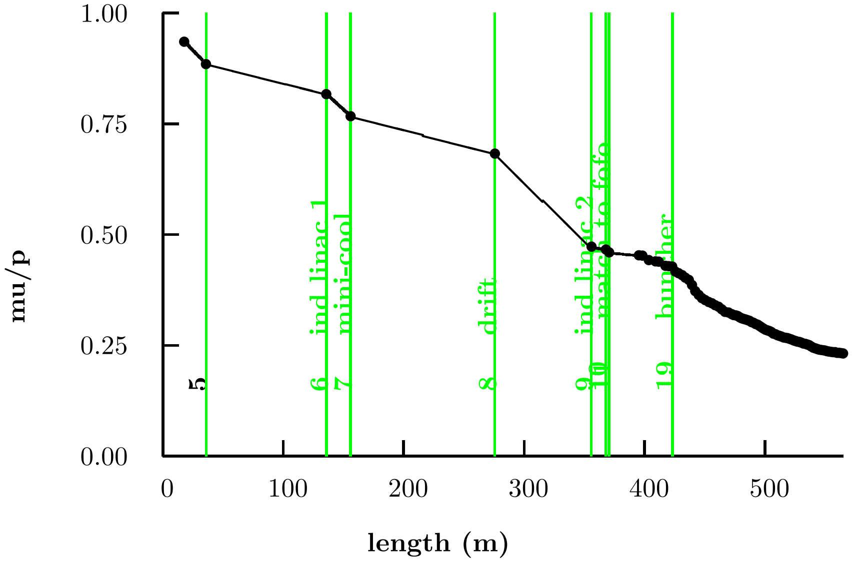


The next figure show the distributions of initial pion energies for (black) all pions exiting the target and (blue) those pions that decayed to muons exiting the cooling. The following figure gives the ratios of these two and indicates that about 35 % of the pions at their peak yield muons at the end, and a falling efficiency for higher energy pions.

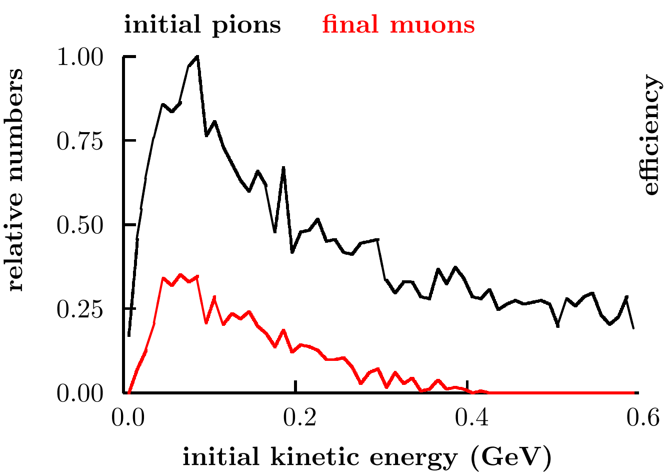


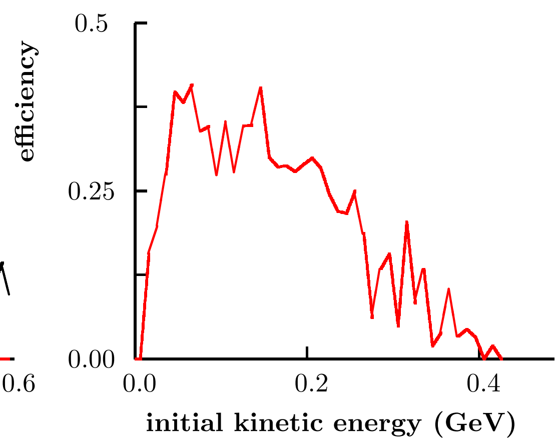

### 3.5 Performance Dependences

We have studied some dependencies of muon production on system parameters:

#### 3.5.1 RF cavity aperture

In this study only the largest RF windows' apertures and thicknesses were changed. The 25 mm apertures were chosen, and are given in the specifications above.

| maximum aperture | thickness | $\mu$/p | | |
|---|---|---|---|---|
| cm | $\mu$m | tot | 15 mm | 9.75 |
| 30 | 500 | .253 | 0.21 | .175 |
| 25 | 250 | .249 | 0.204 | .168 |
| 21 | 125 | .224 | 0.189 | .160 |

#### 3.5.2 proton bunch length

In this study only the proton rms bunch length was changed. It is seen that there is relatively little gain for pulse lengths less than 3 ns, and this is the specified value.

| rms bunch length | $\mu$/p | | |
|---|---|---|---|
| ns | tot | 15 mm | 9.75 |
| 1 | .249 | 0.204 | .168 |
| 3 | .234 | 0.20 | .164 |
| 6 | .204 | 0.167 | .138 |
| 9 | .178 | .144 | .117 |

The above two dependencies are plotted below:

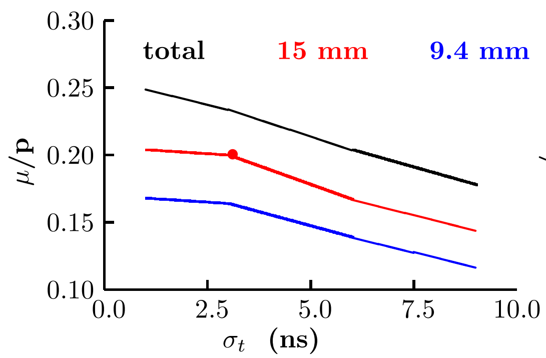


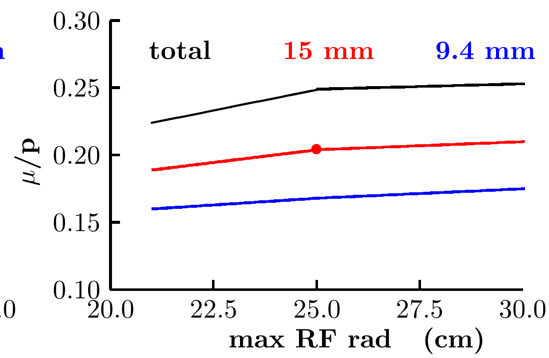

### 3.5.3 target material & proton energy

For comparison with Feasibility Study 1, we have run the program with a carbon target (80 cm long, at 50 mrad) and 16 GeV proton energy. These are given below together with the study 1 values.

| | p energy GeV | rms bunch length ns | $\mu$/p 15 mm | $\mu$/p 9.75 |
|---|---|---|---|---|
| Mercury | 24 | 3 | 0.20 | .164 |
| Carbon | 16 | 3 | .069 | .057 |
| Carbon (Study 1) | 16 | 3 | | .018 |

So the gain over Study 1 from the capture and cooling design improvements is 3.2 $\times$; the gain from the use of the mercury target is 1.9 $\times$; and from the use of a larger accelerator acceptance is 1.2 $\times$; for a total gain of 7.4 $\times$. It should be noted that other authors have also reported cooling schemes with efficiencies substantially greater than those in the Feasibility Study 1. It is believed, never the less, that the scheme proposed here has significant advantages.

# 4 Summary of To be Dones

Simulation tasks that need work include:

- Design periodic focusing channel for long drifts.
- Determine the required rf and hydrogen window thicknesses.
- Design the cavities and simulate.
- Try a third lattice with shorter cell, higher fields and yet lower beta.
- Simulate windows of AlBemet and/or tapered thicknesses.
- Study effects of random errors and set tolerances.
- Study effects of wake fields and space charge.
- Study theoretical assumptions about large angle scatters.
- Add RF near target for polarization.
- Look at trade-offs of induction linac and cooling lengths with performance.
- Add Emittance Exchange.